Imaging Microelectrodes with High-Frequency Electrogenerated Chemiluminescence

R. Mark Wightman,*,† Corrine L. Curtis,† Paul A. Flowers,‡ Russell G. Maus,† and Erin M. McDonald†

Department of Chemistry, University of North Carolina at Chapel Hill, Chapel Hill, North Carolina 27599-3290, and Physical Science Department, University of North Carolina at Pembroke, Pembroke, North Carolina 28732-1510

Received: July 8, 1998; In Final Form: September 15, 1998

The chemiluminescence arising from reaction of electrogenerated intermediates of 9,10-diphenylanthracene (DPA) has been used to generate images of microelectrodes with dimensions in the micrometer range. The experimental conditions were optimized to ensure high luminescent intensity with sharp focusing of the reaction zone to enable good optical resolution. The solution employed, benzonitrile (BN) containing 0.1 M tetrabutylammonium hexafluorophosphate, promotes high intensity because it enables dissolution of a high concentration (>25 mM) of DPA. In addition, radical anions of BN can serve as a reagent reservoir to ensure efficient reaction of DPA radical cations to the singlet excited state. Under these conditions the measured intensity was 3.2×10^5 photons/s per μm^2 of electrode area with a 1 kHz square-wave excitation. Lateral resolution is controlled by the use of rapid potential pulses that maintain the reaction zone in close proximity to the electrode. The images reveal that the electrode areas have quite different topography than inferred from steady-state cyclic voltammograms.

Electrogenerated chemiluminescence (ECL) arises from the production of excited electronic states by chemical reactions of species generated at electrodes.[1] Interest in these processes has spanned almost four decades because these reactions provide routes for chemical systems that can be used in applications such as imaging, chemical analysis, and display devices. Due in large part to the research of Allen J. Bard and co-workers, the mechanisms of light production are now quite well understood. Indeed, his research group has produced more than 37 papers concerning the elucidation of ECL reactions and demonstrating their use in a variety of applications. For example, publications from his group have clarified reaction sequences,[2,3] demonstrated reaction mechanisms,[4] introduced new compounds into the family of ECL emitters,[6] and demonstrated their utility in practical applications.[7,8]

A particularly useful feature of ECL is that it allows visualization of the functional area of an electrode. For example, Engstrom and co-workers showed that the chemiluminescence arising during the oxidation of luminol could be used to observe the time-dependent evolution of uniform flux at a disk microelectrode, present at short times, to the edge-dominated flux that occurs at long times.[9] A similar approach has been used to examine active sites for electron transfer on carbon electrodes.[10−12] Microscopic characterization of the geometry and surface area of microelectrodes is important for interpretation of measured results,[13,14] especially in the case of kinetic measurements made at such electrodes.[15−18] High resolution can be achieved with ECL imaging if the light-emitting species is formed close to the electrode.

Imaging applications of ECL require systems that generate high intensity. Thus, an ideal chemical system for such an application would have a high efficiency of photons produced/electron and would employ high concentration of reagents to maximize the emission intensity. Certain ECL reactions that produce light as a result of annihilation reactions of radical anions and cations have been shown to have very high efficiencies. For example, the annihilation reaction of 9,10-diphenylanthracene (DPA) radical ions approaches 0.25 in dimethoxyethane solvent with low concentrations of supporting electrolyte.[19] An advantage of systems that produce ECL by annihilation reactions is that the original reagents are regenerated and depletion does not occur. When high-speed potential pulses are used, the reaction layer from which light is emitted remains close to the electrode giving high spatial resolution.[20] Furthermore, high-speed generation discriminates against side reactions that can shorten the device lifetime by causing electrode filming.

In this paper we explore the use of high-speed potential pulses as a route to imaging microelectrode surfaces via ECL. As the ECL emitter we have chosen DPA because of its high efficiency. As solvent we have chosen benzonitrile (BN). This solvent has the advantage that it will dissolve high concentrations of DPA, and yet it has sufficient viscosity and conductivity properties to render it useful as a practical electrochemical solvent. As will be shown, it has the additional advantage that it is reducible to a stable radical anion. This property allows it to serve as a reservoir of high-energy electrons to facilitate and accelerate the rate of photon production.

Experimental Section

Apparatus. ECL was characterized in a flow injection analysis system.[20] The system consisted of a stainless steel syringe pump, loop injector, and a channel-type electrochemical cell with a channel height of 150 μm. The floor of the channel was fabricated from epoxy into which was embedded a band or disk-shaped microelectrode. Also embedded in the epoxy was a silver band that served as a pseudo-reference electrode. The ceiling of the channel contained an optical window. A Hamamatsu (Bridgewater, NJ) R5600P photomultiplier tube

* To whom correspondence should be addressed. FAX (919)962-2388, E-mail rmw@unc.edu.
† University of North Carolina at Chapel Hill.
‡ University of North Carolina at Pembroke.

10.1021/jp982913+ CCC: $15.00
Published on Web 10/21/1998

(PMT) operated at −800 V (Pacific, model 204, Concord, CA) was placed adjacent to this window. The output of the PMT was amplified (EGG Ortec VT120A, Oak Ridge, TN) and directed to a multichannel scaler (EGG Ortec T-914). The working electrode was connected to a fast current to voltage converter built in house, and the electrochemical signals were recorded with a digital oscilloscope (Tektronix TDS 380, Wilsonville, OR). The cell potential was controlled with an arbitrary waveform generator (Hewlett-Packard 33120A, Englewood, CO).

Solvents were delivered from the pump to the electrochemical cell at a flow rate of 200 μL/min, and the solutions for ECL or cyclic voltammetric examination were introduced to the cell with the loop injector. For ECL generation the potential waveform was a continuous, 1 kHz square wave unless otherwise noted. The potential limits of the square wave were at least 200 mV beyond the $E_{1/2}$ values of each of the redox couples using the values determined from cyclic voltammograms. In this way, the production of ECL was diffusion limited. PMT counts were binned at 100 kHz for each cycle of the square wave, and the sum of 1000 responses was summed (1 s collection total). To measure the spectral response, an optical fiber bundle (Oriel model 77538, Stratford, CT) was placed between the flow cell window and a JY Optical Systems (H-20, Metuchen, NJ) monochromator, with a 2 nm band-pass, followed by the PMT. ECL emission spectra were obtained by setting the MCS dwell time equal to the speed of the wavelength scan controller (200 nm/min). Spectra were corrected for the wavelength dependence of the PMT sensitivity.

Microscopic Imaging. The imaging system consisted of an inverted stage microscope (Zeiss Axiovert 100 TV, Thornwood, NY) with an electrochemical cell placed over the objective (32×, n/a 0.4, Zeiss). By moving a mirror under the microscope objective, photons could either be collected by a Hamamatsu R4632 PMT or directed to eyepieces and a color CCD camera (768 × 494 picture elements, Sony model SSC-C374, Sony Security Systems, Montvale, NJ). The camera output was sent to a color monitor (Sony model PVM-1350) and a conventional video cassette recorder. The PMT was operated at −800 V (Bertan series 230, Hicksville, NY). Its output was directed to a preamplifier and multichannel scaler as in the flow system. In some experiments the microelectrode was mounted in a scanning tunneling microscope scanner (STM, Topometrix Explorer with scanner model 5370-00, Santa Clara, CA). The scanner has an $x-y$ range of 130 μm in each direction and a z range of 10 μm. Movement of the scanner was used to calibrate the dimensions of the recorded images.

A black felt-covered Plexiglas box enclosed the microscope stage. The electrochemical cell was a glass dish. The counter electrode was a Ag wire (Goodfellow, Cambridge, UK) with a diameter of 0.25 mm and length of 1 cm. Argon was used to purge the box at least 30 min before introduction of the solution of interest. The solution of interest was introduced into the cell with a syringe needle. The same needle was used to deliver argon saturated with the solvent to the headspace immediately above the solution. A potential square wave was directed to the cell from a waveform generator. A digital oscilloscope (Lecroy 9450, Chestnut Ridge, NY) was used to monitor the waveforms.

Conical Microelectrodes. Microelectrodes suitable for electrochemical use in the STM scanner were prepared from Pt/Ir wires (Goodfellow, 90/10 and 80/20 Pt/Ir, Cambridge, U.K.) with a diameter of 0.25 mm using the method described by Bard and co-workers.[21] The tip was immersed approximately 2 mm in a solution of acidic calcium chloride (60% saturated $CaCl_2$, 36% H_2O, 4% HCl). The tip was etched with an ac current (initially 500 mA) applied between the Pt/Ir wire and a graphite rod immersed in the same solution. This procedure produces electrodes with an aspect ratio of approximately 2.

The tips were insulated by translation through molten polyethylene (linear low density, melt index 100, Aldrich, Milwaukee, WI) with an inchworm translator (CE-1000 control module, Burleigh, Fishers, NY) at a speed of 150 μm/s. The molten polyethylene was maintained in an Ω-shaped copper wire loop attached to and heated with a soldering gun in a manner similar to that described by Heben et al.[22] The length of the tip that was coated with polyethylene was approximately 8 mm. The thickness of the polymer coating ranged from vanishingly small at the tip to approximately 0.5 mm (total outside diameter of the electrode was 1 mm). In most cases, this procedure totally insulated the tip. An electroactive area region was exposed by bringing the point of the electrode into contact with an abrasive wheel on a micropipet beveler for a short (∼1 s) time.

For placement in the scanner, the wire was cut to a length of 1.1 cm. This allowed 3 mm of bare Pt/Ir to be inserted into the STM scanner. The electroactive area of the tips was determined from the limiting current during steady-state cyclic voltammetry of 1 mM ferrocene in acetonitrile containing tetrabutylammonium hexafluorophosphate.[21] Electrochemical measurements at varying depths of tip immersion were used to demonstrate that the insulation was devoid of defects or cracks along the sides of the tip.

Chemicals. Acetonitrile (UV grade, Burdick and Jackson, Muskegon, MI) and benzonitrile (HPLC grade, Aldrich,) were used as received. Ferrocene (Aldrich) was sublimed. 9,10-Diphenylanthracene (DPA, Aldrich) was recrystallized twice from absolute ethanol. Tetrabutylammonium hexafluorophosphate (TBAH, Aldrich) was recrystallized twice from 95% ethanol. DPA-containing solutions were deoxygenated with solvent saturated nitrogen before use.

Results

Electrochemical Characteristics of DPA in Benzonitrile. Benzonitrile has several characteristics that make it a suitable solvent for high-speed electrochemistry. Its dielectric constant of 25.9 ensures solubility of salts. Its viscosity,1.267 cP at room temperature, mitigates against excessive solvent loss during bubbling with inert gases. It has a specific resistivity (ρ) of 480 Ω·cm for a solution containing 0.1 M tetrabutylammonium perchlorate.[23] Well-sealed microelectrodes exhibited double-layer capacitance values of approximately 15 μF cm^{-2}. The time constant of an electrochemical cell (RC) with a disk-shaped microelectrode can be estimated by

$$\mathrm{RC} = (\rho/4r)(15 \times 10^{-6})A = 15 \times 10^{-6}\pi\rho r/4$$

where A and r are the disk's area and radius, respectively. Thus, for a 5 μm radius disk, the cell time constant will be approximately 3 μs. This means that electrochemical waveforms with frequencies up to 20 kHz should be little distorted in this solvent.

The emission spectrum of the fluorescence of DPA in BN was found to be identical to that in acetonitrile with an estimated efficiency that was 90% of that in acetonitrile. The diffusion coefficient for DPA in BN containing 0.1 M TBAH, 4.3×10^{-6} cm^2 s^{-1}, was determined from the limiting current for the oxidation during steady-state voltammetry with a 4.6 μm radius, disk-shaped electrode. Fast-scan cyclic voltammograms (1600 V s^{-1}) of 25 mM DPA in this solvent reveal reversible one-

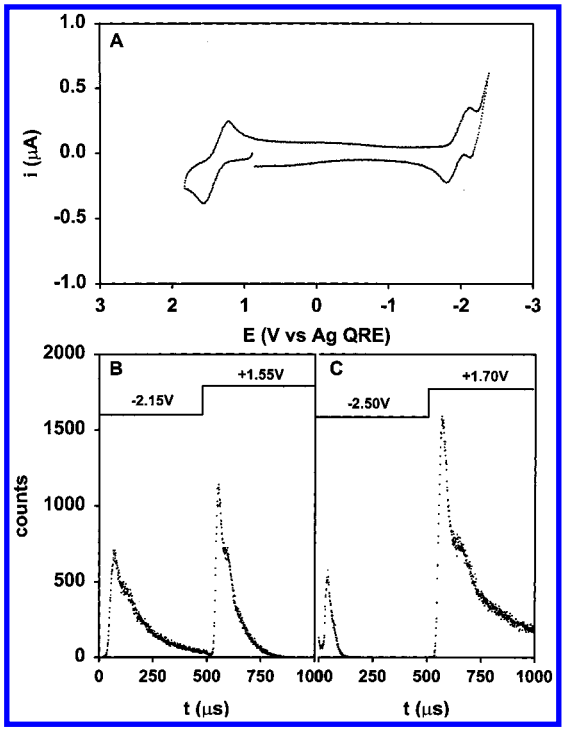

Figure 1. Electrochemical responses of 25 mM DPA in a BN/0.1 M TBAH solution at a 5 μm Au disk electrode measured in the flow injection apparatus. (A) Cyclic voltammetry (scan rate 1600 V/s). (B) ECL time course during potential steps sufficient to generate the radical anion and cation of DPA. (C) ECL time course during potential steps sufficient to generate DPA radical cation and BN radical anion. The traces in panels B and C were recorded with a neutral density filter (OD = 2) between the electrode and PMT. The counts are in 1 μs bins and summed over 1000 potential cycles.

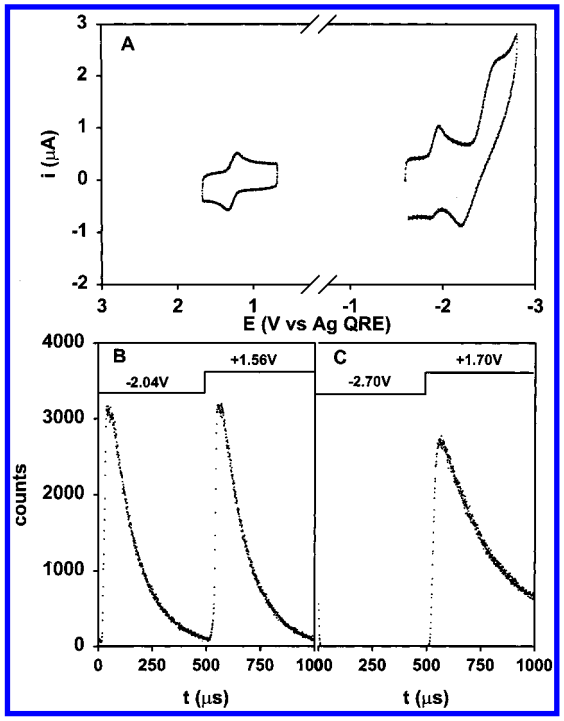

Figure 2. Electrochemical responses of 1 mM DPA and 10 mM BN in an acetonitrile/0.1 M TBAH solution at an Au disk electrode (r = 30 μm). (A) Cyclic voltammetry (scan rate 440 V/s). (B) ECL time course of during potential steps sufficient to generate the radical anion and cation of DPA. (C) ECL time course during potential steps sufficient to generate DPA radical cation and BN radical anion. The traces in panels B and C were recorded with a neutral density filter (OD = 2) between the electrode and PMT. The counts are in 1 μs bins and summed over 1000 potential cycles.

electron oxidation and reduction waves for DPA electrolysis to its radical cation and anion, respectively (Figure 1A). The difference in free energy between the couples ($\Delta E_{1/2}$ = 3.36 V) is sufficient to produce the first excited singlet state of DPA (3.06 eV).[24] However, the reduction of DPA in this solvent lies near the potential limit.

To examine this in more detail, the electrochemistry of DPA (1 mM) was examined in acetonitrile containing 10 mM BN and 0.1 M TBAH. In this solvent $\Delta E_{1/2}$ for DPA is 3.15 V. A quasi-reversible wave can be seen for BN at a potential 500 mV more negative than the first reduction wave for DPA (Figure 2A). Indeed, prior work has shown that the radical anion of BN is quite stable.[25]

ECL from DPA in Benzonitrile. When the radical cation and anion of DPA are alternately generated in acetonitrile with a high-frequency (1 kHz) square wave, light is generated during each potential step as a result of an annihilation reaction between the radical ions (Figure 2B). For example, on the negative step the radical anion diffuses away from the electrode and reacts with the radical cation generated on the previous step, and the reaction produces photons.[26] Thus, for this type of reaction symmetric light transients are expected on each step. Initially, the light intensity is high as the radicals meet in a reaction layer near the electrode. As time evolves, the reaction layer moves further from the electrode and the light decays. The total number of photons/second collected in acetonitrile with the conditions of Figure 2B, adjusted for the presence of the neutral density filter, is 1×10^8. This high value is due in part to the high ECL efficiency for DPA, defined as the number of photons produced/electron passed, which is 6.1% in acetonitrile.[27]

In the acetonitrile containing 10 mM BN, the pattern of light generation is altered when the potential is stepped sufficiently negative to generate BN radical anions (Figure 2C). Under these conditions, light is only generated on the positive going step, and the light does not decay as much during the step. This pattern is that obtained when the ECL reagents have different concentrations.[28] This occurs because generation of BN radical anions provides an excess of negatively charged reagents that can consume the DPA radical cations as they are generated (Figure 2C). The total number of photons during both steps decreased to 72% of that generated in the $DPA^{\bullet+}/DPA^{\bullet-}$ case.

Similar behavior was observed for ECL from 25 mM DPA in BN containing 0.1 M TBAH. When the potentials were stepped to values such that only DPA radical cations and anions were produced, emission peaks with approximately equal amplitude and area are seen on each step (Figure 1B). When the negative potential is increased (holding the positive step at the same value), the emission during the positive step increases and the light on the negative step decreases (Figure 1C) as was the case in acetonitrile-containing benzonitrile. With a 4.2 V potential difference, the total light emission was increased by 1.4-fold compared to that obtained with potential steps only sufficient to generate the DPA radical anion. The total number of detected counts at 1 kHz, normalized by electrode area, is 320 000 photons/μm^2 in benzonitrile with 25 mM DPA. Thus, the intensity in this solution is 9-fold greater than for the conditions shown in Figure 2B. The potential dependence was further examined for 1 mM solutions of DPA (Figure 3A). The intensity was found to diminish with very negative potential steps. An ECL emission spectrum from 1 mM DPA in BN closely matches that for ECL from DPA in acetonitrile (Figure 3B).

Imaging of Electrodes. Images of microelectrode surfaces were examined with an inverted stage microscope during

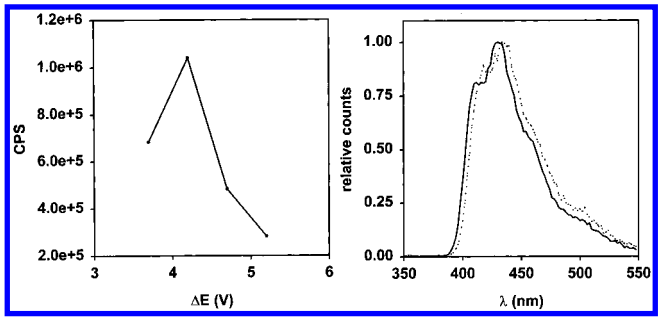

Figure 3. (A) Plot of counts per second (CPS) versus the difference in applied potentials of the square wave (ΔE) for 1 mM DPA in BN containing 0.1 M TBAH. The potential of the positive step was held constant at +1.7 V vs an Ag wire pseudo-reference electrode while the potential of the negative step was increased from −2.0 to −3.5 V. (B) ECL emission spectrum taken for 1 mM DPA in two different solvents. Solid line: acetonitrile/0.1 M TBAH solution obtained with a 30 μm radius Au disk at 1 kHz with potentials of 1.7 and −2.0 V. Dotted line: BN/0.1 M TBAH solution obtained with a 3 μm Au band and potentials of +1.70 and −2.30 V at 1 kHz. Counts were collected in 30 ms bins for 1 pass at 200 nm/min.

generation of ECL in BN containing 25 mM DPA and 0.1 M TBAH. The limits of the applied square-wave potential were adjusted to maximize the ECL intensity. In each experiment the PMT/multichannel scaler system was used to characterize the light emission profiles during each potential step. The light intensity during continuous ECL generation was found to be stable with less than 10% variation for more than 2 h, the longest period of time tested. Also, changes in ECL intensity were not observed while the electrode was moved at scan rates up to 50 μm s^{-1} with the piezoelectric motors of the STM scanner.

The electrode dimensions were determined electrochemically and then compared to the ECL images obtained with the microscope. The electrochemical procedure was to determine the radius by steady-state voltammetry in acetonitrile containing 1 mM ferrocene and 0.1 M TBAH. For an electrode with a disk geometry and located in an infinite insulating plane, the disk radius (r) is given by

$$r = i_d/(anFDC) \quad (1)$$

where i_d is the limiting current, n is the number of electrons per mole, F is the Faraday constant, D is the diffusion coefficient for ferrocene,[29] a is equal to 4, and C is the concentration.

The upper left image of Figure 4 is a bright-field image of the electrode tip. The electrode was a platinum disk electrode sealed in a large glass tube such that it has a large region of insulation surrounding the metal.[30] The image is a front end view of the electrode with the electroactive area closest to the observer and the rest of the electrode extending away. When

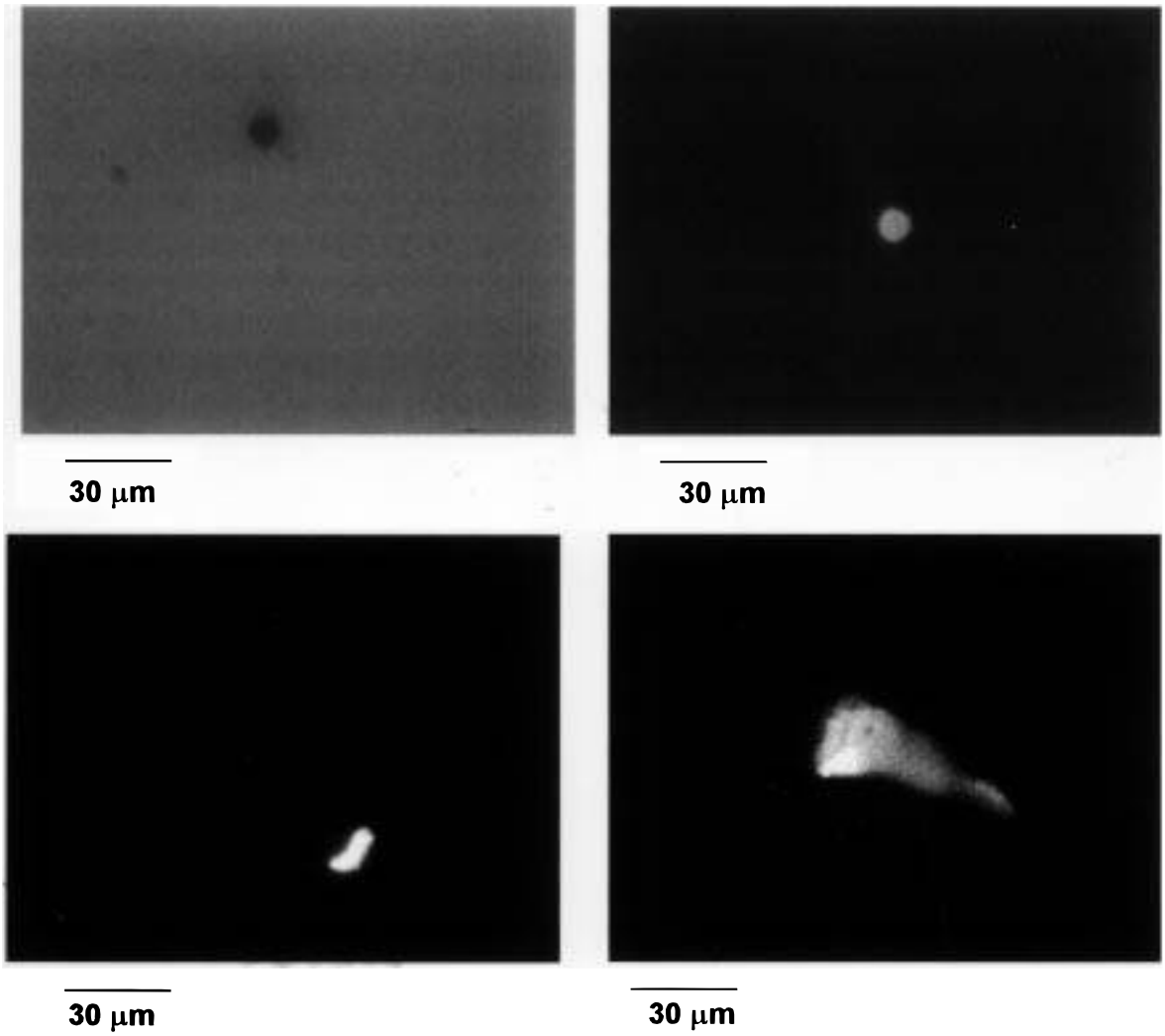

Figure 4. ECL images of microelectrodes in benzonitrile containing 25 mM DPA and 0.1 M TBAH. Upper panels: results from a Pt disk electrode (5.6 μm radius determined electrochemically) sealed in a large glass insulator and polished. Left: bright-field image. Right: ECL image generated with a 1 kHz square wave; the measured counts were 3.7×10^6/s. Lower panels: conical electrodes whose tips were briefly polished on a beveling wheel. Distance bars determined with STM scanner.

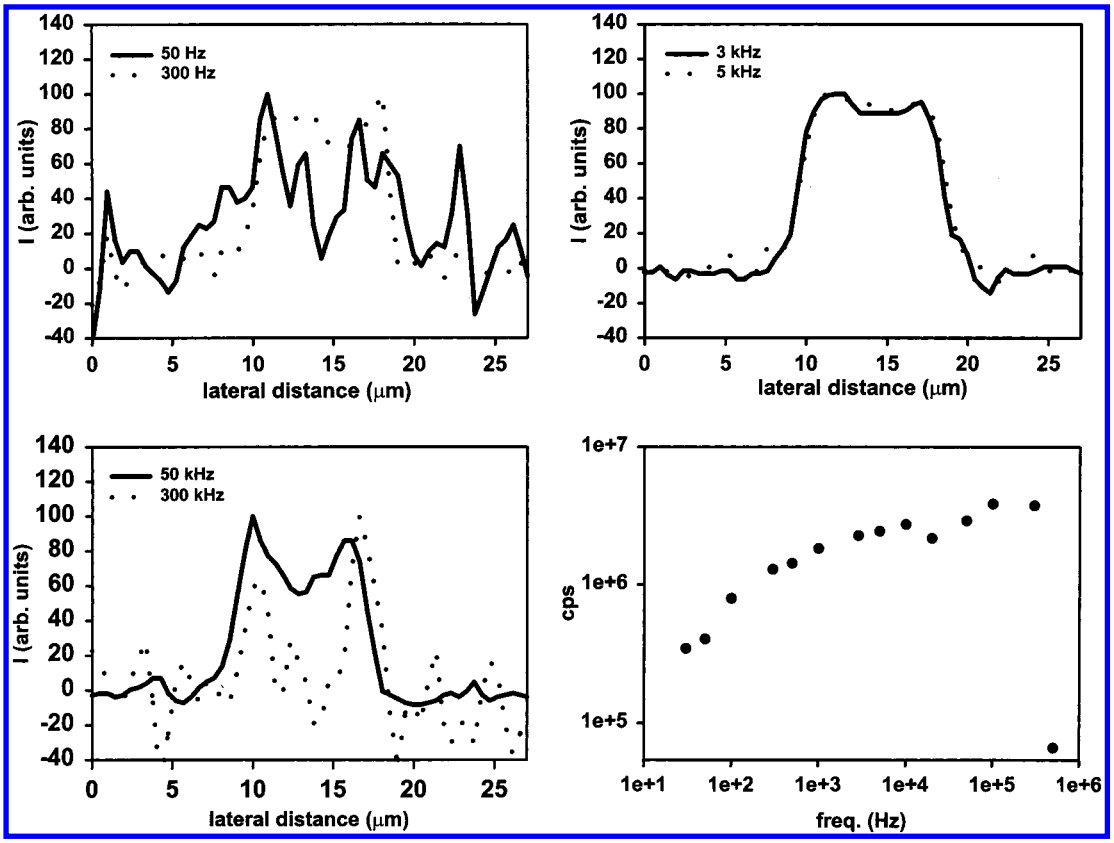

Figure 5. Cross-section intensities from ECL generated at a 5.6 μm radius, disk-shaped electrode at different frequences. Data were obtained from video recordings of the CCD camera images. In each case above 10 kHz, the potentials were increased to give maximal intensities. The intensities have been normalized; the cumulative intensities measured with the PMT are shown in the bottom right panel.

examined by electron microscopy, such electrodes exhibit a geometry that is approximately that of a disk. The ECL image from the same electrode is shown in the upper right of Figure 4. The radius determined electrochemically was 5.6 μm, whereas that obtained from the area of the ECL image of the electrode was 4.7 μm.

Similar characterization was done for conical microelectrodes insulated with polyethylene and mounted in the STM scanner. For example, the image shown in the lower left of Figure 4 was obtained from an electrode that had been briefly beveled. For an electrode that has a very thin layer of insulation at the tip, the *a* term in eq 1 has a larger value and approaches 6 for an infinitely thin insulator.[31,32] Using this value, a radius of 7.2 μm was obtained from the steady-state electrochemical current (it was identical before and after the ECL imaging). The ECL image yielded an area that was equivalent to that of a disk with a 6.5 μm radius. The agreement is quite good despite the fact that it is clear from the ECL image that the electrode does not have a disk geometry. In most cases beveling of the electrodes resulted in bent tips as evidenced by the ECL image that appears as a hooklike structure (Figure 4, lower).

The resolution of the technique was examined by evaluating the cross-sectional intensity across a $r = 5$ μm electrode (Figure 5). Measurements at intermediate frequencies (500 Hz−10 kHz) reveal that the measured intensity at the edges rises over approximately 1 μm, which corresponds to the estimated pixel resolution with the objective used. At the lowest frequency shown (50 Hz) the light intensity is dimmer in the center of the electrode, and it appears to spread further from the outer circumference of the electrode. At low frequencies radial diffusion to the electrode occurs, leading to a higher flux of radicals generated at the perimeter. In addition, reagents must diffuse further to find a reaction partner that was generated on the previous step. These combined effects lead to an expectation of a lowered spatial resolution and a greater intensity near the perimeter.

As the frequency is increased, the ohmic drop caused by the charging current becomes larger, and the amplitude of the applied square wave must be increased to obtain maximal light intensity. When this is done at frequencies above 30 kHz, the luminescence at the perimeter again becomes enhanced. We attribute this to an effect termed the primary current distribution,[33] which refers to flux of electrolyte moving toward and away from the electrode on alternate half-cycles of the square wave. Just as diffusing molecules at low frequency can reach the perimeter more easily than the center of the disk because they can approach from the side as well as from a direction normal to the electrode, electrolyte ions moving to the electrode surface also find it easier to reach the perimeter. This effect is only seen when ionic movement, rather that electron-transfer kinetics or diffusion, is the chief cause of the impedance of the electrochemical cell.

Discussion

The results of this paper show that the ECL generated at high frequencies from DPA in BN is ideal for imaging purposes. The intensity is high and the spatial resolution is good. Furthermore, the chemical system is stable for a considerable period of time, allowing comprehensive examination of surfaces. The images obtained with this approach provide more information concerning the geometry of the microelectrode than that obtained from voltammetric measurements alone. Indeed, the results reveal that the electrodes constructed using simple techniques have quite bizarre shapes and certainly cannot be considered disks. The responses of such electrodes would be

difficult to fit to theoretical predictions for the flux and thus would be unsuitable for kinetic measurements.

The high intensity observed in this work is obtained because high concentrations are used with a system that regenerates the starting materials. Because ECL increases directly with concentration, BN was selected as solvent since it enables dissolution of greater concentrations of DPA than can be employed in the more commonly used acetonitrile (DPA solubility limit ~1 mM). ECL from the DPA radical anion/cation system could be obtained in BN as in acetonitrile. However, it was found that this solvent was also advantageous in that BN's electrogenerated radical anion can provide a reservoir of reagents for light production via reaction with the radical cation of DPA. Enabling this reservoir by stepping to more negative potentials caused a considerable increase in the light intensity, and the spectral features reveal the emission is from the singlet excited state of DPA. With even larger potential differences the emission decreased, presumably because the radical anion of BN absorbs in the region of DPA emission.[34] Thus, when generated at high concentrations, it can reduce the photon flux. The approximate 9-fold increase in the light output for the typically used conditions in BN (as in Figure 1C) relative to that in acetonitrile is equivalent to the product of the ratio of the concentrations and the ratio of the square root of the diffusion coefficients, a result anticipated for diffusion-controlled ECL generation if the efficiencies are similar in the two solvents.[20]

The high ECL intensity is also a consequence of the high-frequency generation employed. ECL normally increases with the square root of the applied potential frequency.[20] The optimum frequencies for imaging, between 1 and 20 kHz, were selected after evaluating the factors that can effect the sensitivity. With very low frequencies radial diffusion at microelectrodes carries electrogenerated species away from the electrode. As well as lowering the probability of undergoing a light-producing reaction, this diffusion compromises the lateral resolution of the technique. However, at very high frequencies, spatially nonuniform luminescence is also observed. It appears that the intensity at the perimeter is enhanced because this is the region that can most rapidly establish the ionic gradient necessary to maintain the potential gradient required to generate radical ions.

Under conditions where the light-producing reaction is rapid, as with the high concentrations used in this work, the light-emitting zone is a thin plane that is parallel to the electrode surface, which moves away as time elapses.[26] The movement of this plane away from the reflective surface of the electrode causes constructive and destructive interference of the emission due to the interaction with its reflectance from the electrode.[35] This is manifested in this work as the oscillations superimposed on the measured emission curves. For example, in the DPA radical anion/cation annihilation system in BN operated at a 1 kHz frequency, the light emitting zone at 150 μs into each step is 360 nm from the electrode surface, whereas the wavelength of maximal emission is at 440 nm. For the conditions employed with the BN radical anion, this reaction layer will be even closer to the surface because the electrogenerated DPA radical cation is more likely to find a reaction partner. If the singlet excited state is generated too close to the electrode (~50 nm), it can be quenched by interaction with the metallic surface. This is another factor that limits the useful upper frequency limit of the technique.

The reported intensity for 25 mM DPA in BN with a step-potential frequency of 1 kHz, 3×10^5 photons/(s μm^2) is very high for chemiluminescent systems. For example, a recent paper by Bard and co-workers shows 90 photons/(s μm^2) generated with the ruthenium tris(bipyridine)/tripropylamine system in acetonitrile at a microelectrode.[36] Of course, the measured intensity also depends on the efficiency of collection of photons. In the flow injection apparatus used in this work this is estimated to be 5%.[37] Thus, an estimated 6×10^6 photons/(s μm^2) is generated by the ECL reaction. This is more than sufficient to observe by eye the emission from an electrode with a radius as small as 1 μm when mounted on the microscope and allows clear resolution of very small active sites on electrodes.

Acknowledgment. This research was supported by the National Science Foundation.

References and Notes

(1) Faulkner, L. R.; Bard, A. J. In *Electroanalytical Chemistry*; Bard, A. J., Ed.; Marcel Dekker: New York, 1977; Vol. 10, pp 1−95.
(2) Wallace, W. L.; Bard A. J. *J. Phys. Chem.* **1979**, *83,* 1350−1357.
(3) Faulkner, L. R.; Tachikawa, H.; Bard, A. J. *J. Am. Chem. Soc.* **1972**, *94*, 691−699.
(4) Richards, T. C.; Bard, A. J. *Anal. Chem.* **1995**, *67*, 3140−3147.
(5) Xu, X.-H.; Bard, A. J. *J. Am. Chem. Soc.* **1995**, *117*, 2627−2631.
(6) Debad, J. D.; Morris, J. C.; Lynch, V.; Magnus, P.; Bard, A. J. *J. Am. Chem. Soc.* **1996**, *118*, 2374−2379.
(7) Laser, D.; Bard, A. J. *J. Electrochem. Soc.* **1975**, *122*, 632−640.
(8) Brilmeyeer, G. H.; Bard, A. J. *J. Electrochem. Soc.* **1980**, *127*, 104−110.
(9) Pharr, C. M.; Engstrom, R. C.; Tople, R. A.; Bee, T. K.; Unzelman, P. L. *J. Electroanal. Chem.* **1990**, *278*, 119−128.
(10) Engstrom, R. C.; Johnson, K. W.; DesJarlais, S. *Anal. Chem.* **1987**, *59*, 670−673.
(11) Bowling, R. J.; McCreery, R. L.; Pharr, C. M.; Engstrom, R. C. *Anal. Chem.* **1989**, *61*, 2763−2766.
(12) Hopper, P.; Kuhr, W. G. *Anal. Chem.* **1994**, *66*, 1996−2004.
(13) Mirkin, M. V.; Fan, F. R. F.; Bard, A. J. *J. Electroanal. Chem.* **1992**, *328*, 47−62.
(14) Fang, Y.; Leddy, J. *Anal. Chem.* **1995**, *67*, 1259−1270.
(15) Penner, R. M.; Heben, M. J.; Longin, T. L.; Lewis, N. S. *Science* **1990**, *250*, 1118−1120.
(16) Baranski, A. S.; Winkler, K.; Fawcett, W. R. *J. Electroanal. Chem.* **1991**, *313*, 367−375.
(17) Baranski, A. S. *J. Electroanal. Chem.* **1991**, *307*, 287−292.
(18) Oldham, K. B. *Anal. Chem.* **1992**, *64*, 646−651.
(19) Maness K. M.; Wightman, R. M. *J. Electroanal. Chem.* **1995**, *396*, 85−96.
(20) Collinson, M. M.; Wightman, R. M. *Anal. Chem.* **1993**, *65*, 2576−2582.
(21) Gewirth, A. A.; Cranston, D. H.; Bard, A. J. *J. Electroanal. Chem.* **1989**, *261*, 477.
(22) Heben, M. J.; Dovek, M. M.; Lewis, N. S.; Penner, R. M.; Quate, C. F. *J. Microsc.* **1988**, *152*, 651.
(23) Kadish, K. M.; Ding, J. Q.; Malinski, T. *Anal. Chem.* **1984**, *56*, 1741.
(24) Beldeman, F. E.; Hercules, D. M. *J. Phys. Chem.* **1979**, *83,* 2203−2209.
(25) Rieger, P. H.; Bernal, I.; Reinmuth, W. H.; Fraenkel, G. K. *J. Am. Chem. Soc.* **1963**, *85*, 683.
(26) Pastore, P.; Magno, F.; Collinson, M. M.; Wightman, R. M. *J. Electroanal. Chem.* **1995**, *397*, 19−26.
(27) Manness, K. M.; Bartelt, J. E.; Wightman, R. M. *J. Phys. Chem.* **1994**, *98*, 3993−3998.
(28) Ritchie, E. L.; Pastore, P.; Wightman, R. M. *J. Am. Chem. Soc.* **1997**, *119*, 11920−11925.
(29) Baur, J. E.; Wightman, R. M. *J. Electroanal. Chem.* **1991**, *305*, 73−81.
(30) Wightman, R. M.; Wipf, D. O. In *Electroanalytical Chemistry*; Bard, A. J., Ed.; Marcel Dekker: New York, 1988; Vol. 15; Chapter 3, pp 267−353.
(31) Shoup, D.; Szabo, A. *J. Electroanal. Chem* **1984,** *160*, 27−31.
(32) Fang, Y.; Leddy, J. *Anal. Chem.* **1995**, *67*, 1259−1270.
(33) Newman, J. *J. Electrochem. Soc.* **1966**, *113*, 501−502.
(34) Shida, T. *Electronic Absorption Spectra Of Radical Ions;* Elsevier: Amsterdam, 1988; p 239.
(35) Collinson, M. M.; Pastore, P.; Maness, K. M.; Wightman, R. M. *J. Am. Chem. Soc.* **1994**, *116*, 4095−4096.
(36) Collinson, M. M.; Wightman, R. M. *Science* **1995**, *268*, 1883−1885.
(37) Fan, F. F.; Cliffel, D.; Bard, A. J. *Anal. Chem.* **1998**, *70*, 2941−2948.